

Thermally Induced Fluctuations below the Onset of Rayleigh-Bénard Convection

Mingming Wu, Guenter Ahlers, and David S. Cannell

Department of Physics and Center for Nonlinear Science, University of California, Santa Barbara, California 93106

(Received 7 November 1994)

We report quantitative experimental results for the intensity of noise-induced fluctuations below the critical temperature difference ΔT_c for Rayleigh-Bénard convection. The structure factor of the fluctuating convection rolls is consistent with the expected rotational invariance of the system. In agreement with predictions based on stochastic hydrodynamic equations, the fluctuation intensity is found to be proportional to $1/\sqrt{-\epsilon}$, where $\epsilon \equiv \Delta T/\Delta T_c - 1$. The noise power necessary to explain the measurements agrees with the prediction for thermal noise.

PACS numbers: 47.20.-k, 43.50.+y, 47.54.+r

Bifurcations in spatially extended dissipative systems are usually discussed in terms of deterministic equations for the macroscopic variables which neglect thermal noise. Many such “ideal” systems undergo a sharp bifurcation at a critical value of a control parameter, where a spatially uniform state loses stability and a state with spatial variation appears. However, if noise is present, it will drive the system to fluctuate away from the uniform state, even below the bifurcation. As near a thermodynamic critical point, the fluctuation amplitudes grow as the bifurcation is approached because the susceptibility diverges there. Using the stochastic hydrodynamic equations introduced by Landau and Lifshitz [1], this problem was considered theoretically over two decades ago [2–4] for the case of Rayleigh-Bénard convection (RBC), which is the buoyancy-induced motion in a shallow horizontal layer of fluid heated from below. For RBC the deterministic model predicts pure conduction until the temperature difference ΔT exceeds a critical value ΔT_c . In the presence of noise, time-dependent fluctuating flows are predicted to occur even for $\Delta T < \Delta T_c$. They have zero mean, but their root-mean-square amplitude is finite. This amplitude diverges at ΔT_c when nonlinear saturation is neglected. These fluctuations induced by thermal noise were expected to be unobservably weak because the thermal energy $k_B T$ which drives them is many orders of magnitude smaller than the typical kinetic energy of a macroscopic convecting fluid element.

In this Letter, we report experimental measurements of fluctuations below ΔT_c in a large-aspect-ratio convection cell [5,6]. Using the shadowgraph technique, we observed fluctuating convection rolls of random orientation. Their structure factor consisted of a ring without significant angular variation. The mean square fluctuation amplitude was found to increase as $\epsilon \equiv \Delta T/\Delta T_c - 1$ approached zero, within experimental resolution proportional to $1/\sqrt{-\epsilon}$. These experimental results agree with predictions based on the Navier-Stokes equations with additive noise terms [1]. The noise power necessary to explain the amplitude agrees well with the value calculated by van Beijeren and Cohen (vBC) [7,8] for thermal noise with rigid boundaries.

The only previous measurement of thermal fluctuations in a hydrodynamic system suitable for comparison [9] with theory of which we are aware is due to Rehberg *et al.* [10] and involved electroconvection in a nematic liquid crystal (NLC). Even though that system is “macroscopic,” it is particularly susceptible to noise because the physical dimensions are only of order $10 \mu\text{m}$ and because the elastic constants, which determine the macroscopic energy to which $k_B T$ has to be compared, are exceptionally small. In a NLC there is a preferred direction, and thus electroconvection and RBC belong to different symmetry classes. The measurements reported here reveal the effect of the rotational invariance in the horizontal plane of the RBC system on its fluctuations.

We used a circular cell [11] filled with CO_2 at pressures of 28.96, 31.02, and 42.33 bars, held constant to $\pm 10^{-4}$ bar. The cell height was $d = 468$ (481) μm , and the aspect ratio (radius/height) was 85 (83) at 28.96 (31.02 and 42.33) bars. The top and bottom plates were 0.953 cm thick optically flat sapphire disks whose temperatures were held constant to ± 0.3 mK. Using interferometry, we found d to be constant to $\pm 0.15 \mu\text{m}$ over the central 80% of the cell radius. The sidewall was made of paper. The top and bottom plate temperatures were adjusted so as to keep their mean fixed at 32.00°C . The density [12] ρ , isobaric thermal expansion coefficient [12] α , heat capacity [13] C_P , shear viscosity [14] η , and thermal conductivity [15] λ are given in [16]. The vertical thermal diffusion time $t_v \equiv d^2/\kappa$ ($\kappa = \lambda/\rho C_P$) was near 1 s, and typical fluctuation lifetimes are given by $t_l = t_v \tau_0/|\epsilon|$ with [17] $\tau_0 \simeq 0.07$. The Prandtl number $\sigma \equiv \nu/\kappa$ (ν is the kinematic viscosity) was 0.91, 0.92, and 1.04 at 28.96, 31.02, and 42.33 bars, respectively. When ΔT exceeded ΔT_c , a transcritical bifurcation from the conduction state to convection in the form of hexagons occurred [11]. At 28.96, 31.02, and 42.33 bars, we found ΔT_c to be 23.56, 17.27, and $5.46 \pm 0.002^\circ\text{C}$, and we changed ϵ in steps of 8×10^{-5} , 1×10^{-4} , and 4×10^{-4} , respectively. Throughout this paper, length will be scaled by d .

The fluctuating flows were visualized by the shadowgraph technique [18–20]. The light beam passed through the cell twice vertically, being reflected from the bot-

tom plate. Images contained 256×256 pixels and covered an area $2.5 \text{ cm} \times 2.5 \text{ cm}$ located in the interior of the cell. A time series of 128 background images was taken at $\Delta T_c = 2.0^\circ \text{C}$ at time intervals large compared to t_l . Each of these images was the average of 16 images taken 0.44 s apart. Here the fluctuations were extremely weak, but to further reduce their contribution the average $\tilde{I}_0(\mathbf{x})$ of the 128 images was used as the background image (\mathbf{x} is the horizontal position). After this, ΔT was ramped up slowly to $\epsilon \approx -0.006$, where the fluctuations became large enough to measure. A series of 64 images $\tilde{I}_i(\mathbf{x}, \epsilon)$ was taken (again each image was an average of 16 taken 0.44 s apart) at each of many ϵ values for $-0.006 \leq \epsilon < 0$. These were used to compute the signal image

$$I_i(\mathbf{x}, \epsilon) = [\tilde{I}_i(\mathbf{x}, \epsilon) - \tilde{I}_0(\mathbf{x})]/\tilde{I}_0(\mathbf{x}). \quad (1)$$

Before each image sequence at a new ϵ value, the system was equilibrated for 1 h. The time between successive images was kept approximately equal to t_l so the measurements were nearly uncorrelated. In obtaining the amplitude of the fluctuations a small ($\leq 20\%$) ϵ -dependent correction was made to account for the effect of averaging 16 images for each final image.

Ideally, for $\epsilon < 0$, the flow would consist only of fluctuations. However, imperfections in the cell caused *deterministic* flow. Although the imperfections were *extremely* small, their relative influence increased as the bifurcation was approached from below because the deterministic flow velocity grows as $|\epsilon|^{-1/2}$, whereas that of the fluctuations grows only as $|\epsilon|^{-1/4}$. Consequently, near the transition even a microscopic dust particle can force flow in the form of concentric rings [11], which may contribute to a shadowgraph image. In one case, the sample area of interest contained one or two such particles, and for $|\epsilon| \geq 10^{-4}$ the fraction of the sample influenced by them was small. In the parameter range of interest the velocities are so small that the system is linear. Thus superposition is valid, and the deterministic signal could be identified by averaging all the signal images $I_i(\mathbf{x}, \epsilon)$ taken at a given ϵ . It could then be removed by subtracting this average from each signal image taken at that ϵ . Figure 1(a) shows a grey-scale rendition of such a difference image $\delta I(\mathbf{x}, \epsilon)$, for $\epsilon = -3.0 \times 10^{-4}$. It reveals some spatial variation in excess of instrumental noise, but the detailed structure of the fluctuating flow is hard to discern. Figure 1(b) is a grey-scale rendition of $|\delta I(\mathbf{q}, \epsilon)|^2$, where $\delta I(\mathbf{q}, \epsilon)$ is the spatial Fourier transform of $\delta I(\mathbf{x}, \epsilon)$. A dark ring is apparent, indicating that the fluctuations can be considered as superimposed convection rolls with many different orientations and a preferred wave number q_0 . Figure 1(c) is taken barely above the onset (nominally $\epsilon = 0$). The image shows a defect-free hexagonal pattern [11]. The modulus squared of its Fourier transform is displayed in Fig. 1(d). Notice that the hexagon wave number is essentially the same as the radius q_0 of the ring in Fig. 1(b).

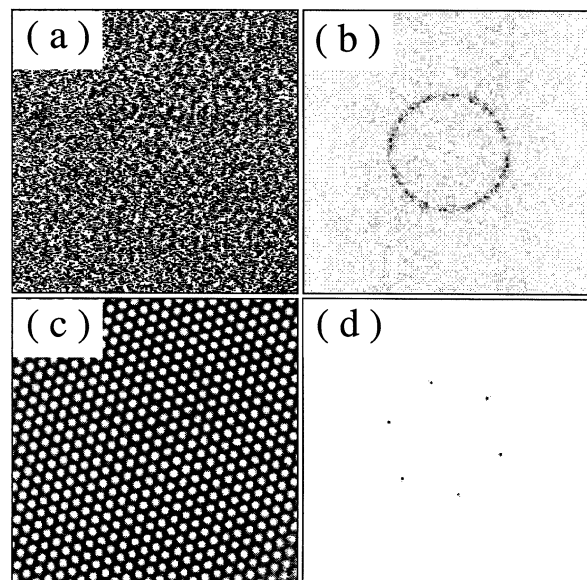


FIG. 1. Grey-scale images. (a) Shadowgraph image of fluctuating rolls, at a pressure of 28.96 bars, for $\epsilon = -3.0 \times 10^{-4}$. (b) Square of the modulus of the Fourier transform of the image in (a). (c) Shadowgraph image of a hexagonal pattern, at a pressure of 28.96 bars, for $\epsilon \approx 0$. (d) Square of the modulus of the Fourier transform of the image in (c).

In order to measure the mean square amplitude of the fluctuations as accurately as possible, we averaged 64 Fourier images of the sort shown in Fig. 1(b), at each ϵ , to give the structure factor $S(\mathbf{q}, \epsilon) \equiv \langle |\delta I(\mathbf{q}, \epsilon)|^2 \rangle$. The results at several ϵ are shown in Fig. 2. The structure factor shows no obvious azimuthal variation, and thus reflects the underlying rotational invariance of the RBC system [21]. As ϵ approached zero, the rings became darker, showing that the fluctuations become stronger as the system approaches the deterministic onset. The azimuthal average of $S(\mathbf{q}, \epsilon)$, which we denote $S(q, \epsilon)$, is shown in Fig. 3. Although deterministic contributions have been eliminated, it still has a smooth ϵ -independent background $S_B(q)$ due to camera noise and other effects. Separately at each ϵ , we included $S_B(q)$ in fitting the experimental data for $S(q)$, modeling $S_B(q)$ as $B_0 + B_1 q^2 + B_2 q^4$. The solid lines are fits by the function

$$S(q, \epsilon) = \frac{S_0}{(q - q_0)^2 + \Gamma^2} \left(\frac{q}{q_0} \right)^4 + S_B(q), \quad (2)$$

which should pertain [7,22] close to threshold, where the fluctuating temperature field is expected to be approximately Lorentzian in q space. The background is shown as the dashed line. Equation (2), with S_0 , q_0 , Γ , and B_i adjustable, was found to provide an excellent fit to the data for all pressures and ϵ studied. The factor of $(q/q_0)^4$ is necessary to relate the shadowgraph signal to the temperature fluctuations as discussed below.

For comparison with theory, the quantity of interest is the mean square amplitude of $\delta T(\mathbf{x}, z, \epsilon)$, the fluctuation in the temperature field, which can be written as $\delta T(\mathbf{x}, \epsilon) \hat{\theta}_0(z)$, where the vertical eigenfunction $\hat{\theta}_0(z)$

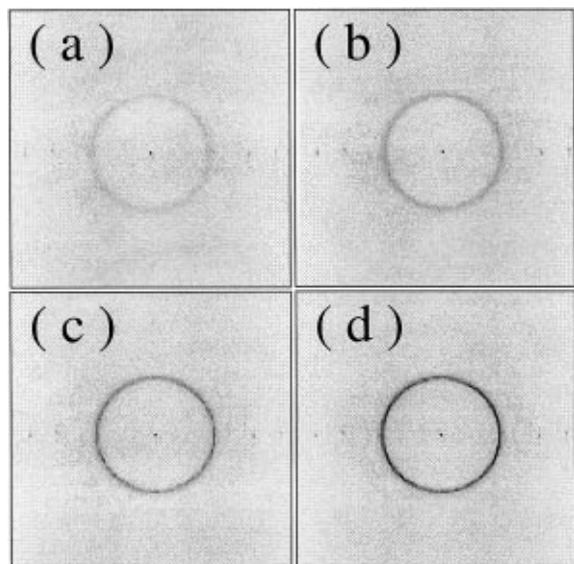


FIG. 2. Grey-scale images of the structure factor for gas convection in CO_2 at a pressure of 28.96 bars at each of four ϵ values. (a) $\epsilon = -4.2 \times 10^{-3}$, (b) $\epsilon = -1.6 \times 10^{-3}$, (c) $\epsilon = -7.1 \times 10^{-4}$, (d) $\epsilon = -3.0 \times 10^{-4}$.

is normalized so that its square integrates to unity (see Eq. A24b of Ref. [21]). For our experimental setup, the shadowgraph signal $\delta I(\mathbf{q}, \epsilon)$ and the temperature fluctuation $\delta T(\mathbf{q}, \epsilon)$ are directly proportional [19,20]:

$$\delta I(\mathbf{q}, \epsilon) = G \left(\frac{q}{q_0} \right)^2 \delta T(\mathbf{q}, \epsilon). \quad (3)$$

The constant G can be written as $2\gamma(z_1) \times q_0^2 z_1 (\partial n / \partial T) \langle \tilde{\theta}_0(z) \rangle_z$. Here z_1 is the optical distance from the cell to the imaging plane, n is the refractive index of the fluid, the vertical average $\langle \tilde{\theta}_0(z) \rangle_z$ is equal to 0.8892, and $\gamma(z_1)$ is a numerical factor which may be computed [20] on the basis of physical optics, and which for our geometry is equal to 0.89. Parseval's theorem then allows the mean square amplitude of the fluctuations $\delta T^2(\epsilon) \equiv \langle [\delta T(\mathbf{x}, \epsilon)]^2 \rangle_x$ to be obtained by

integrating the Lorentzian portion of the structure factor of the shadowgraph signal:

$$\delta T^2(\epsilon) = 2\pi G^{-2} \int_0^\infty q \left[\frac{S_0}{(q - q_0)^2 + \Gamma^2} \right] dq. \quad (4)$$

For a Lorentzian, the integral diverges. This problem arises from the truncation involved [23] in calculating the temperature fluctuations. In their evaluation of the results of vBC, Hohenberg and Swift (HS) made the approximation

$$\int_0^\infty \frac{q dq}{(q - q_0)^2 - \Gamma^2} \approx q_0 \int_0^\infty \frac{dq}{(q - q_0)^2 - \Gamma^2} \quad (5)$$

(see Eq. A16 of HS) in order to avoid this problem. Equation (5) can be justified [23] to lowest order in ϵ on the basis of the exact result of Zaitsev and Shliomis [2].

It is clearly a good approximation at small $|\epsilon|$ where $S(q, \epsilon)$ has a small width, and making the same approximation in the data analysis yields

$$\delta T^2(\epsilon) = 2\pi^2 G^{-2} S_0 q_0 / \Gamma. \quad (6)$$

By making this same approximation, we expect that corrections of higher order in ϵ will cancel to a large extent in the comparison with theory. Figure 4 gives the results for $\delta T^2(\epsilon)$ obtained from the fitting parameters using Eq. (6) as a function of ϵ at two pressures. The solid lines are fits to the data using the theoretical result $\delta T^2 = A/\sqrt{-\epsilon}$. The adjustable parameters were the amplitude A and ΔT_c . The results for ΔT_c were typically very slightly larger (by a few parts in 10^4) than the value at which a hexagonal pattern first appeared, suggesting a slightly premature transition in the presence of the fluctuations. The statistical errors derived from the fits were typically a few percent, but we expect that systematic errors from various sources may increase the uncertainty of A to somewhere between 10% and 20%.

The amplitudes of the fluctuating modes below but close to onset were calculated by vBC [7] (Eqs. 9, 10b, and 12b of vBC), using realistic (no-slip) boundary conditions at the top and bottom of the cell, but they

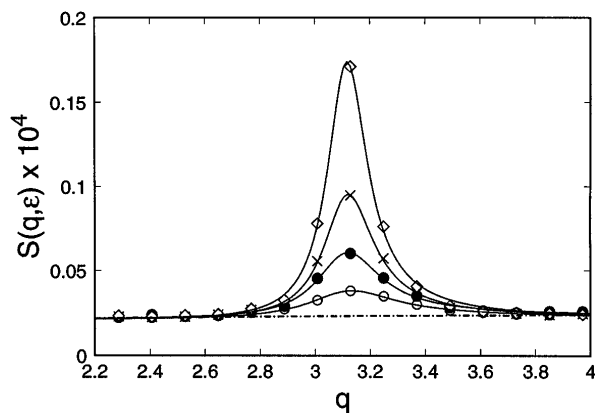


FIG. 3. Azimuthal integral $S(q, \epsilon)$ of the structure factor $S(\mathbf{q}, \epsilon)$ as a function of q for various ϵ at a pressure of 28.96 bars. \circ , $\epsilon = -4.2 \times 10^{-3}$; \bullet , $\epsilon = -1.6 \times 10^{-3}$; \times , $\epsilon = -7.1 \times 10^{-4}$; \diamond , $\epsilon = -3.0 \times 10^{-4}$.

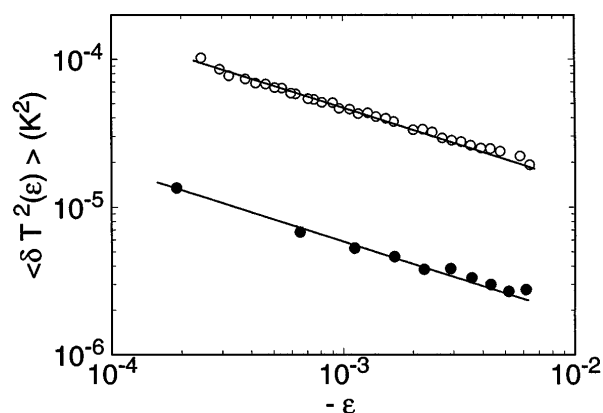


FIG. 4. The variance $\delta T^2(\epsilon)$ of the temperature fluctuations as a function of ϵ on logarithmic scales. \bullet , $P = 42.33$ bars; \circ , $P = 28.96$ bars. The solid lines are fits of $\delta T^2(\epsilon) = A/\sqrt{-\epsilon}$ to the data.

TABLE I. Comparison of F^{th} with F^{expt} .

P (bars)	ΔT_c^{expt}	$10^7 F^{\text{expt}}$	$10^7 F^{\text{th}}$
28.96	23.56	2.60	2.31
28.96	23.56	2.71	2.31
31.02	17.27	3.60	2.48
42.33	5.46	6.41	4.09

did not calculate $\delta T^2(\epsilon)$. They did, however, compute (Eq. 16 of vBC) the quantity $\mathcal{N} - 1$, where the Nusselt number \mathcal{N} is the ratio of the effective conductivity in the presence of convective fluctuations to the conductivity in the absence of such fluctuations. As shown by HS, $\mathcal{N} - 1$ is related to $\delta T^2(\epsilon)$ by (Eq. 2.12 of HS)

$$\delta T^2(\epsilon) = \tilde{c}^2 \left(\frac{\Delta T_c}{R_c} \right)^2 (\mathcal{N} - 1), \quad (7)$$

with $\tilde{c} = 3q_0\sqrt{R_c}$. They also evaluated the results of vBC for $\mathcal{N} - 1$ for the case of an infinite system very near threshold, obtaining

$$\mathcal{N} - 1 = \frac{F^{\text{th}}}{4\sqrt{-\epsilon}}, \quad (8)$$

where F^{th} is a dimensionless thermal noise power given by

$$F^{\text{th}} = \frac{k_B T}{\rho d \nu^2} \frac{2\sigma q_0}{\xi_0 \tau_0 R_c}, \quad (9)$$

with $q_0 = 3.117$, $\xi_0 = 0.385$, $\tau_0 = 0.0796$, and $\sigma = \nu/\kappa$ the Prandtl number. We may thus compare the experimental results for $\delta T^2(\epsilon)$ to the theoretical prediction by defining an experimental noise power through

$$\delta T^2(\epsilon) = \tilde{c}^2 \left(\frac{\Delta T_c}{R_c} \right)^2 \frac{F^{\text{expt}}}{4\sqrt{-\epsilon}},$$

with F^{expt} being determined by the fits to the data for $\delta T^2(\epsilon)$.

In Table I we compare F^{th} with F^{expt} . For the measurements made at 28.96 bars, the ratio of F^{expt} to F^{th} is 1.15, while it is about 1.5 for the measurements made at higher pressures. We have no explanation for this apparent difference, but note that the shadowgraph signals at the higher pressure were weaker and thus accurate measurements more difficult. We thus conclude that the experimental noise power is, within our resolution, very nearly equal to the theoretical estimate [2,7] for thermal noise based on the stochastic hydrodynamic equations [1].

The authors wish to thank Eberhard Bodenschatz, Pierre Hohenberg, Stephen Morris, Steve Trainoff, and Maurice M.H.P. van Putten for valuable discussions. This work was supported by the Department of Energy through Grant No. DE-FG03-87ER13738.

[1] L.D. Landau and E.M. Lifshitz, *Fluid Mechanics* (Addison-Wesley, Reading, MA, 1959).

[2] V.M. Zaitsev and M.I. Shliomis, Zh. Eksp. Teor. Fiz. **59**, 1583 (1970) [Sov. Phys. JETP **32**, 866 (1971)].

- [3] R. Graham, Phys. Rev. A **10**, 1762 (1974).
- [4] J.B. Swift and P.C. Hohenberg, Phys. Rev. A **15**, 319 (1977).
- [5] Qualitative observations of fluctuations were reported previously in Ref. [6].
- [6] E. Bodenschatz, S. Morris, J. de Bruyn, D.S. Cannell, and G. Ahlers, in *Proceedings of the KIT International Workshop on the Physics of Pattern Formation in Complex Dissipative Systems*, edited by S. Kai (World Scientific, Singapore, 1992), p. 227.
- [7] H. van Beijeren and E.G.D. Cohen, J. Stat. Phys. **53**, 77 (1988).
- [8] In principle, the more recent calculations for binary mixtures by W. Schöpf and W. Zimmermann [Phys. Rev. E **47**, 1739 (1993)] should also yield the noise power for pure fluid, but a detailed evaluation for our Prandtl number has not yet been carried out.
- [9] Recent measurements on binary-mixture convection by W. Schöpf and I. Rehberg [Europhys. Lett. **17**, 321 (1992); J. Fluid Mech. **271**, 235 (1994)] and by G. Quentin and I. Rehberg (private communication) involved pseudo-one-dimensional sample geometries for which no theoretical predictions exist at present.
- [10] I. Rehberg, S. Rasenat, M. de la Torre-Juarez, W. Schöpf, F. Hörner, G. Ahlers, and H.R. Brand, Phys. Rev. Lett. **67**, 596 (1991).
- [11] E. Bodenschatz, J. de Bruyn, G. Ahlers, and D.S. Cannell, Phys. Rev. Lett. **67**, 3078 (1991).
- [12] M.P. Vukalovich and V.V. Altunin, *Thermophysical Properties of Carbon Dioxide* (Collet's, London, 1968).
- [13] S. Angus, B. Armstrong, K.M. de Reuck, V.V. Altunin, O.G. Gadetskii, G.A. Chapela, and J.S. Rowlinson, *International Thermodynamic Tables of the Fluid State Carbon Dioxide* (Pergamon, Oxford, 1976).
- [14] H. Iwasaki and M. Takahashi, J. Chem. Phys. **74**, 1930 (1981).
- [15] J.V. Sengers, Ph.D. thesis, University of Amsterdam, 1962 (unpublished).
- [16] We used Eq. 5.68 of Ref. [12] to get ρ and α , Table 3 of Ref. [13] for C_p , the results of Ref. [14] for the shear viscosity η , and the data of Ref. [15] for the thermal conductivity λ . For $P = 28.96, 31.02, \text{ and } 42.3$ bars, we used $10^2 \rho = 5.899, 6.411, 9.551$ g/cm³, $10^3 \alpha = 5.50, 5.76, 7.64$ K⁻¹, $10^4 \eta = 1.57, 1.58, 1.63$ P, $\lambda = 1932, 1960, 2156$ ergs/(s cm K), and $C_p = 1.114, 1.145, \text{ and } 1.379$ J/g K, respectively.
- [17] M.A. Dominguez-Lerma, G. Ahlers, and D.S. Cannell, Phys. Fluids **27**, 856 (1984).
- [18] See, for instance, V. Steinberg, G. Ahlers, and D.S. Cannell, Phys. Scr. **32**, 534 (1985).
- [19] S. Rasenat, G. Hartung, B.L. Winkler, and I. Rehberg, Exp. Fluids **7**, 412 (1989).
- [20] S. Trainoff, D.S. Cannell, and G. Ahlers (to be published).
- [21] Early experiments [6] revealed that the azimuthal uniformity of $S(\mathbf{q}, \epsilon)$ can be spoiled by a very small angle between the top and bottom plates. Only an extremely parallel alignment yields the azimuthal symmetry revealed in Fig. 2.
- [22] P.C. Hohenberg and J.B. Swift, Phys. Rev. A **46**, 4773 (1992).
- [23] J.B. Swift and P.C. Hohenberg (private communication).